

# Effects of microwave power on the structural and emission properties of hydrogenated amorphous silicon carbide deposited by electron cyclotron resonance chemical vapor deposition

J. Cui, Rusli,<sup>a)</sup> S. F. Yoon, M. B. Yu, K. Chew, J. Ahn, and Q. Zhang

*School of Electrical and Electronic Engineering, Nanyang Technological University, Nanyang Avenue, Singapore 639798, Republic of Singapore*

E. J. Teo, T. Osipowicz, and F. Watt

*Research Centre for Nuclear Microscope, Physics Department, National University of Singapore, 10 Kent Ridge Crescent, Singapore 119260*

(Received 11 August 2000; accepted for publication 1 December 2000)

Hydrogenated amorphous silicon carbide ( $a\text{-Si}_{1-x}\text{C}_x\text{:H}$ ) films have been deposited using an electron cyclotron resonance chemical vapor deposition system. The effects of varying the microwave power from 100 to 1000 W on the deposition rate, optical band gap, film composition, and disorder were studied using various techniques such as Rutherford backscattering spectrometry, spectrophotometry, Fourier-transform infrared absorption, and Raman scattering. Samples deposited at 100 W are found to have a carbon fraction ( $x$ ) of 0.49 which is close to that of stoichiometric SiC, whereas samples deposited at higher microwave powers are carbon rich with  $x$  which are nearly independent of the microwave power. The optical gaps of the films deposited at higher microwave powers were noted to be related to the strength of the C–H<sub>*n*</sub> bond in the films. The photoluminescence (PL) peak emission energy and bandwidth of these films were investigated at different excitation energies ( $E_{\text{ex}}$ ) and correlated to their optical band gaps and Urbach tail widths. Using an  $E_{\text{ex}}$  of 3.41 eV, the PL peak energy was found to range from 2.44 to 2.79 eV, with the lowest value corresponded to an intermediate microwave power of 600 W. At increasing optical gap, the PL peak energy was found to be blueshifted, accompanied by a narrowing of the bandwidth. Similar blueshift was also observed at increasing  $E_{\text{ex}}$ , but in this case accompanied by a broadening of the bandwidth. These results can be explained using a PL model for amorphous semiconductors based on tail-to-tail states radiative recombination. A linear relation between the full width at half maximum of the PL spectra and the Urbach energy was also observed, suggesting the broadening of the band tail states as the main factor that contributes to the shape of the PL spectra observed.

© 2001 American Institute of Physics. [DOI: 10.1063/1.1344218]

## I. INTRODUCTION

Hydrogenated amorphous silicon carbide ( $a\text{-Si}_{1-x}\text{C}_x\text{:H}$ ) films have attracted much attention due to their unique thermal, mechanical, optical, and electronic properties.<sup>1,2</sup> These render them potentially suitable for several innovative device applications, such as visible light emitting diodes,<sup>3</sup> wide band gap window materials for amorphous silicon solar cell,<sup>4</sup> and active layers in large area electroluminescence devices.<sup>5</sup>  $a\text{-Si}_{1-x}\text{C}_x\text{:H}$  is also an interesting material for the basic study of amorphous semiconductors as its structural, optical, and electrical properties can be varied over a wide range through alloying different fractions of Si, C, and H. Typically, it was found that by adjusting the carbon fraction ( $x$ ) from 0.3 to 0.7, optical band gaps ranging from 2 to 3 eV could be obtained.<sup>6</sup>

$a\text{-Si}_{1-x}\text{C}_x\text{:H}$  films have been commonly deposited using rf plasma enhanced chemical vapor deposition (rf-PECVD) technique, and their structural and optical properties have been extensively investigated.<sup>7,8</sup> Although alloying Si with carbon widens the optical band gap of  $a\text{-Si}_{1-x}\text{C}_x\text{:H}$

compared to  $a\text{-Si:H}$ , previous studies have shown that these films prepared by the rf-PECVD technique contained compositional inhomogeneity when incorporated with a higher fraction of carbon due to the presence of  $\pi\text{-}\pi^*$  ( $sp^2$ ) bonded carbon. This results in alloys with lower band gaps and poorer optoelectronic properties which limit their applications in electronic devices.<sup>9,10</sup> In recent years, the electron cyclotron resonance chemical vapor deposition (ECR-CVD) has been increasingly applied as an alternative technique for the growth of various amorphous semiconductors such as  $a\text{-Si:H}$ ,<sup>11</sup>  $a\text{-C:H}$ ,<sup>12</sup>  $a\text{-SiN:H}$ ,<sup>13</sup> and  $a\text{-SiC:H}$ .<sup>14</sup> Compared to the conventional rf plasma, the ECR-microwave plasma has advantages such as higher electron temperature, higher plasma ionization rate, higher ion flux (1–50 mA/cm<sup>2</sup>), and lower deposition pressure and temperature.<sup>13,15</sup> The higher ionization rate leads to the generation of a high density plasma with density in the range of  $10^{11}\text{--}10^{12}\text{ cm}^{-3}$ . Besides, the ion energy and the degree of plasma ionization can be independently controlled through the applied dc or rf-induced bias and the microwave power, respectively. As a result of the above attractive properties, the ECR-CVD technique has also been applied for the deposition of different

<sup>a)</sup>Electronic mail: erusli@ntu.edu.sg

silicon carbide films which include  $a\text{-Si}_{1-x}\text{C}_x\text{:H}$ ,<sup>14,16</sup>  $uc\text{-SiC:H}$ ,<sup>17,18</sup> and doped  $uc\text{-SiC:H}$ .<sup>19,20</sup> These studies however, have concentrated on the effects of gas flow ratio, deposition pressure, and substrate temperature on the properties of the hydrogenated silicon carbide films. In contrast, the effects of the microwave power, which is the main parameter that determines the degree of plasma ionization, on the optical and structural properties of  $a\text{-Si}_{1-x}\text{C}_x\text{:H}$  films have not been widely investigated to date. Previously, we have studied the effects of microwave power and gas pressure on the properties of boron-doped SiC:H films deposited by the ECR-CVD technique.<sup>21,22</sup> In this work, large band gap intrinsic  $a\text{-Si}_{1-x}\text{C}_x\text{:H}$  films grown using the same technique are investigated for optoelectronic applications such as in thin film light emitting diodes. A comprehensive study on the structural, optical, and emission properties of these  $a\text{-Si}_{1-x}\text{C}_x\text{:H}$  films under varying microwave powers will be presented. Interestingly, it is found that strong blue photoluminescence at room temperature can be observed from films with large optical gaps.

## II. EXPERIMENTS

In this work, hydrogenated amorphous silicon carbide thin films were prepared by an ECR-CVD system, the schematic diagram of which can be found elsewhere.<sup>21</sup> The microwave power was guided through a rectangular waveguide and introduced into the ECR magnetron excitation chamber through a quartz window. A magnetic field of approximately 875 G required for the ECR condition can be created within the excitation chamber by using currents of 100 and 120 A for the upper and lower magnetic coils, respectively. The magnetron controls a divergent mirror magnetic field profile that extracts the ECR plasma into the deposition chamber located below the excitation chamber.  $\text{SiH}_4$ ,  $\text{CH}_4$ , and  $\text{H}_2$  are introduced into the deposition chamber through the excitation chamber gas inlet. The ECR condition heats the electrons which ionize the gas to establish and maintain the plasma. All the films were deposited on two different types of substrate simultaneously: (1)  $\langle 100 \rangle$ -oriented single-crystal Si wafers for film thickness, Raman scattering, IR absorption, and photoluminescence measurements and (2) Corning 7095 glass for optical transmittance and reflectance measurements. All the substrates were cleaned in acetone and propanol, rinsed in de-ionized water, and dried in nitrogen ambient, before loading into the vacuum chamber. For all the depositions, the gas flow ratio of  $\text{SiH}_4$  (10% diluted in  $\text{H}_2$ ):  $\text{CH}_4$ : $\text{H}_2$  was set to 10:2:100 sccm. Depositions were carried out with different microwave powers ranging from 100 to 1000 W at 22 mTorr and 30 °C. Neither rf self-bias nor dc bias voltage was applied to the substrate, as this could induce strong ion bombardments leading to films with higher defect density and poorer emission properties.

The carbon fraction  $x$  ( $[\text{C}]/([\text{C}]+[\text{Si}])$ ) in the  $a\text{-Si}_{1-x}\text{C}_x\text{:H}$  films was deduced using Rutherford backscattering (RBS) spectrometry. The optical band gaps of the films were determined by transmittance and reflectance measurements using a dual beam Perkin-Elmer Lambda 16 spectrophotometer. The Tauc band gaps  $E_g$  were extracted

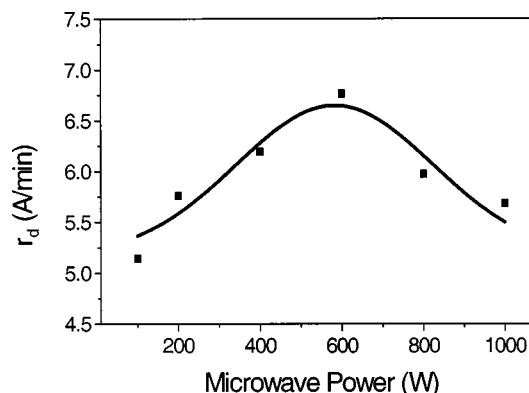


FIG. 1. The deposition rate ( $r_d$ ) as a function of microwave power.

using the Tauc equation  $(\alpha E)^{1/2} = B(E - E_g)$ , where  $B$  is a constant,  $\alpha$  is the absorption coefficient, and  $E$  is the photon energy. However, for samples with higher band gap, it was difficult to determine the Tauc gap unambiguously as the linear region used for fitting the Tauc equation was not wide enough. For this reason the  $E_{04}$  gaps, defined as the energy at which  $\alpha$  is equal to  $10^4 \text{ cm}^{-1}$ , were also determined for all the samples. The Urbach energy  $E_0$  was extracted by fitting the exponential tail of the absorption coefficient curve to  $\alpha = \alpha_0 \exp[(E - E^*)/E_0]$ , where  $\alpha_0$  and  $E^*$  are constants. Infrared absorption measured using a Fourier-transform infrared (FTIR) spectrometer (Perkin-Elmer 2000) in the range from 400 to  $3500 \text{ cm}^{-1}$  was used to study the nature of bonding of  $a\text{-Si}_{1-x}\text{C}_x\text{:H}$  alloys. The Raman spectra were excited using the 244 nm line from a frequency doubled  $\text{Ar}^+$  laser source and collected in a backscattering configuration by a charge coupled device camera using a Renishaw micro-Raman System 2000 spectrometer. Photoluminescence (PL) measurements were carried out at room temperature using an  $\text{Ar}^+$  ion laser directed at near normal incidence to the sample. Several excitation energies  $E_{\text{ex}} = 2.41, 2.49, 2.54, 2.60, 2.71,$  and  $3.41 \text{ eV}$  were used, and the PL spectra were detected using a water-cooled Hamamatsu R2949 photomultiplier tube (PMT) based on single-photon counting technique through a 1/4 m double monochromator Digikrom DK242. The PL spectra were corrected for the combined response of the PMT and monochromator.

## III. RESULTS AND DISCUSSION

Figure 1 shows the deposition rate ( $r_d$ ) as a function of the microwave power. The  $r_d$  initially increases with the microwave power from 100 to 600 W, and then decreases at higher microwave powers. Similar results have been obtained from our previous study on boron-doped  $a\text{-SiC:H}$  film deposition using the ECR-CVD technique.<sup>21,22</sup> The variation of  $r_d$  is believed to be a result of the competition between deposition and hydrogen ion etching. The initial increase was likely due to the enhanced ionization of the ECR plasma under increasing microwave power, leading to more radicals and reactive species being created and, hence, an increase in the deposition rate. When the microwave power was increased beyond 600 W, the available reactive species contributing to the film growth could be limited by the low flow

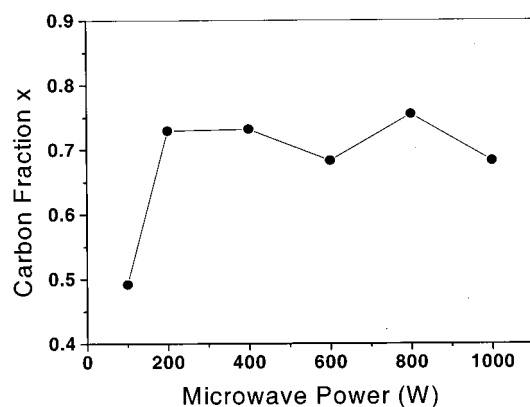


FIG. 2. The carbon fraction  $x$  deduced using RBS as a function of microwave power.

rates of  $\text{SiH}_4$  and  $\text{CH}_4$  (1 and 2 sccm, respectively), despite the high ionization rate of the ECR microwave plasma. On the other hand, due to the high  $\text{H}_2$  dilution, there was a strong dissociation of  $\text{H}_2$  that increased with the microwave power, especially at the higher microwave power range. The large amount of hydrogen atoms could etch off weaker  $sp^2$  bonded carbon incorporated in the films, leading to a decrease in the deposition rate. It is expected that if the flow rates of  $\text{CH}_4$  and  $\text{SiH}_4$  are increased, the maximum deposition rate will also increase and occur at microwave powers higher than 600 W. In this work, it is noted that the maximum  $r_d$  achieved, 6.7 Å/min, is several times lower than that reported by Conde *et al.*<sup>14</sup> This is possibly due to no bias voltage being applied to the substrates during film growth in our case.

Figure 2 shows the carbon fraction  $x$  as a function of the microwave power obtained from RBS measurement. The detailed compositions are shown in Table I. Information on the H fractions in the films is not available in the present study. It is interesting to note that the samples can be classified into two regimes. Those deposited at 100 W (SCJ01) have  $x = 0.49$ , which is very close to that of stoichiometric SiC. The others deposited at higher microwave powers are carbon rich with  $x$  ranging from 0.68 to 0.76. In fact, for microwave power higher than 200 W, the variation in  $x$  is small and almost independent of the microwave power. From the large composition difference observed, it can be deduced that there was an abrupt change in the plasma conditions when the

TABLE I. Compositions of the  $a\text{-Si}_{1-x}\text{C}_x\text{:H}$  films as a function of the microwave power. The gas flow ratio of  $\text{SiH}_4$  (10% diluted in  $\text{H}_2$ ):  $\text{CH}_4\text{:H}_2$  was set to 10:2:100 sccm and the deposition pressure and substrate temperature were kept constant at 22 mT and 30 °C, respectively.

Sample	Microwave power (W)	Carbon fraction ( $x$ )	Silicon fraction ( $1-x$ )
SCJ01	100	0.49	0.51
SCJ02	200	0.73	0.27
SCJ03	400	0.73	0.27
SCJ04	600	0.68	0.32
SCJ05	800	0.76	0.24
SCJ06	1000	0.68	0.32

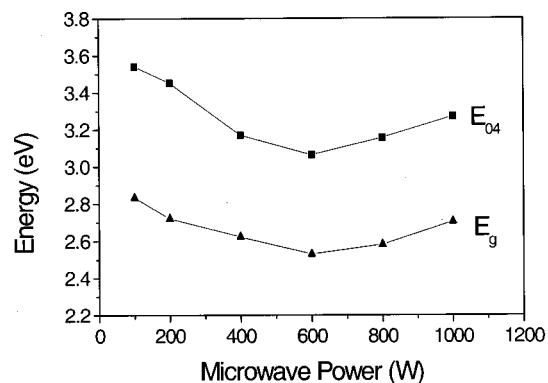


FIG. 3. The optical band gap  $E_{04}$  and  $E_g$  as a function of microwave power.

microwave power was increased from 100 to 200 W. It is noteworthy that under the rf “starving” plasma condition, one can deposit diamond-like  $a\text{-Si}_{1-x}\text{C}_x\text{:H}$  films with high band gap and low defect density using the rf-PECVD technique.<sup>23,24</sup> The starving plasma condition was achieved using lower rf power density which was able to break the Si-H bond (3.4 eV) in  $\text{SiH}_4$  but not the C-H bond (4.2 eV) in  $\text{CH}_4$  due to the difference in their bonding energies. It is proposed that the 100 W microwave power regime in this work resembles this condition of insufficient ionization of  $\text{CH}_4$  resulting in the lower carbon fraction  $x$  observed compared to the other samples. Indeed, the sample SCJ01 deposited at 100 W has been found to have higher band gap and less disorder compared to the other samples, as shall be shown shortly. The relatively small variation in  $x$  for microwave higher than 200 W suggests that in this regime, the microwave power does not significantly affect the relative ionization of  $\text{SiH}_4$  and  $\text{CH}_4$ .

Figure 3 shows the optical bandgap  $E_{04}$  and Tauc gap  $E_g$  as a function of the microwave power. Both the  $E_{04}$  and  $E_g$  gaps have their minimum values at 600 W, and interestingly exhibit a trend with the microwave power that is opposite to that observed for the deposition rate. The optical gaps of these  $a\text{-Si}_{1-x}\text{C}_x\text{:H}$  films depend critically on the fraction of Si and C, besides other factors such as the H fraction and the predominating bonding configurations for the carbon atoms. As carbon can be found in both the trivalent ( $sp^2$ ) and tetravalent ( $sp^3$ ) forms for at least  $x > 0.5$ , the band gap of  $a\text{-Si}_{1-x}\text{C}_x\text{:H}$  films do not follow a monotonic increase with  $x$  but in all cases exhibit a maximum at  $x = x_c \approx 0.65$ .<sup>25</sup> This nonmonotonic behavior of the band gap energy with  $x$  was first explained by Robertson,<sup>26</sup> who showed that below  $x_c$  the band edge is of  $\sigma$ -bonded Si-C  $sp^3$  character, whereas above  $x_c$  it is of  $\pi$ -bonded C=C  $sp^2$  character. As  $x$  is increased the former moves up in energy and the latter down so that at the crossover a maximum appears. In our case, the variation in  $x$  for the samples SCJ02–SCJ06 is small and as such does not account for the change in the band gap observed. In fact, it can be seen in Fig. 3 that the optical gaps obtained in this work are generally quite high, above 3 eV for the  $E_{04}$  gap and above 2.5 eV for the Tauc gap  $E_g$ . The sample SCJ01 ( $a\text{-Si}_{0.51}\text{C}_{0.49}\text{:H}$ ) deposited at 100 W exhibits large optical band gap as a result of the plasma starving condition used as discussed earlier, and also due to its near

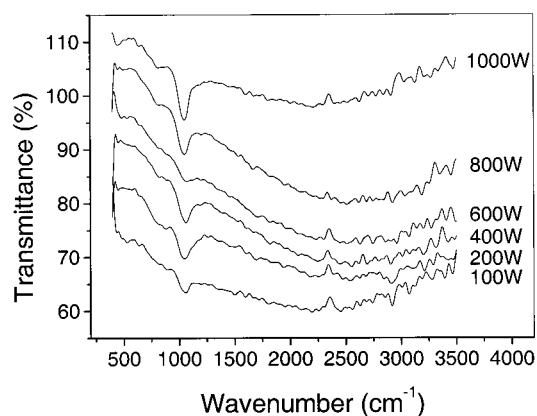


FIG. 4. FTIR transmittance spectra of the  $a\text{-Si}_{1-x}\text{C}_x\text{:H}$  films deposited at different microwave powers.

stoichiometric composition. The other carbon-rich  $a\text{-Si}_{1-x}\text{C}_x\text{:H}$  samples contain large carbon fractions, mainly in polymeric forms as supported by the IR absorption results to be shown later, and account for the large optical gap observed. It is noted that polymeric  $a\text{-C:H}$  films with  $E_{04}$  as high as 4.3 eV have been previously reported by Rusli *et al.*<sup>27</sup> The slight increase in the optical gap for the samples SCJ05 and SCJ06 could be related to abundant H atoms at higher microwave power above 600 W which effectively etched off weaker  $sp^2$  bonded carbon. This is also consistent with the observed variation in the deposition rate with microwave power, as argued earlier.

Figure 4 shows the FTIR spectra for all the films corrected for their different thickness. The dominant mode of vibration in our spectra is around  $1040\text{ cm}^{-1}$ , corresponding to the  $\text{C-H}_n$  ( $n=2,3$ ) wagging mode to which silicon atoms are attached.<sup>28,29</sup> This suggests that the films contain substantial hydrogen. It is noted that the  $\text{Si-C}$  bond around  $800\text{ cm}^{-1}$  can be seen for samples deposited at higher microwave powers, attributed to the stronger hydrogen etching effect at these microwave powers. This helps to etch weaker carbon  $sp^2$  bonds and promotes bonding with silicon atoms to form tetrahedral  $\text{Si-C}$  bond. The  $\text{C-H}_n$  stretching mode at around  $2900\text{ cm}^{-1}$  can be observed for SCJ01 and SCJ02.  $\text{Si-H}$  stretching mode which occurs at  $2100\text{ cm}^{-1}$  are absent in all our films. For samples SCJ02–SCJ06, the large fraction of  $\text{C-H}_n$  wagging mode around  $1040\text{ cm}^{-1}$  is believed to be due to the high concentration of hydrogen used in the deposition. When the microwave power is increased from 200 to 1000 W, the intensity of the  $\text{C-H}_n$  mode at about  $1040\text{ cm}^{-1}$  decreases at first, exhibiting a minimum at 600 W microwave power before increases subsequently, revealing a trend similar to that observed for the optical gaps in Fig. 3. This suggests the optical gaps of  $a\text{-Si}_{1-x}\text{C}_x\text{:H}$  films deposited at microwave power higher than 200 W are dominated by the number of  $\text{C-H}_n$  bond. Sah *et al.*<sup>30,31</sup> have also reported that for rf glow discharge deposited  $a\text{-Si}_{1-x}\text{C}_x\text{:H}$ , there is approximately a proportional relation between the optical gap and the  $\text{Si-CH}_3$  (located around  $770\text{ cm}^{-1}$ ) concentration.

Raman scattering has proved to be useful in detecting the  $\text{Si-Si}$  and  $\text{C=C}$  bonds of the films which are not reveal

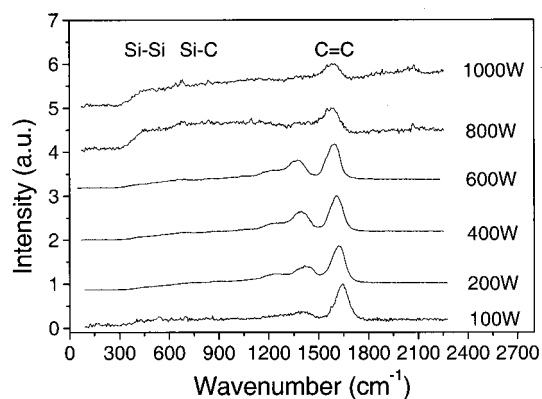


FIG. 5. The Raman scattering spectra of the  $a\text{-Si}_{1-x}\text{C}_x\text{:H}$  samples deposited at different microwave powers.

by infrared absorption due to their symmetrical bonding and absence of dipole moments. The Raman spectra of  $a\text{-Si}_{1-x}\text{C}_x\text{:H}$  have been generally observed to have the following main bands:  $300\text{--}600\text{ cm}^{-1}$  corresponds to the amorphous silicon that is associated with  $\text{Si-Si}$  bond,  $1300\text{--}1600\text{ cm}^{-1}$  corresponds to  $\text{C-C}$  bond associated with amorphous carbon and  $\text{Si-C}$  bond is expected to be in the region of  $650\text{--}1000\text{ cm}^{-1}$ . The Raman spectra for the six samples are plotted in Fig. 5 and are displaced vertically for clarity. It can be seen that for all the samples the  $\text{C-C}$  bonds are clearly seen, which is expected due to the carbon-rich nature of our films and is also consistent with the results of Chehaidar *et al.*<sup>32</sup> For the samples SCJ01–SCJ04, the Raman spectra contain two prominent peaks centered around  $1610$  and  $1390\text{ cm}^{-1}$  which correspond to the characteristic graphite-like  $G$  band<sup>33</sup> and disorder-induced graphite-like  $D$  band,<sup>34</sup> respectively. It can be seen that with the microwave power increased from 100 to 600 W, the intensity of the  $D$  band increases with respect to that of  $G$  band. This has been shown to be correlated to an increase in the  $sp^2$  bonded carbon in the case of diamond-like carbon films.<sup>35</sup> For these four samples, Si related bonds were not observed. On the other hand, for samples SCJ05 and SCJ06, very weak  $\text{Si-Si}$  and  $\text{Si-C}$  bonds can be seen. Choi *et al.*<sup>36</sup> have reported such bonds in the Raman spectra of rf sputtered  $a\text{-Si}_{1-x}\text{C}_x\text{:H}$  films are absent. Anderson and Spear<sup>37</sup> have pointed out the difficulty of detecting the  $\text{Si-C}$  bond by the Raman scattering technique. The bond polarizability of  $\text{C-C}$  is greater than that of  $\text{Si-C}$  by a factor of about 40,<sup>38</sup> and this may explain why only a predominant  $\text{C-C}$  bond was observed in Fig. 5.

The variation in the Urbach tail width  $E_0$  with the microwave power is shown in Fig. 6, where it can be seen that  $E_0$  exhibits a trend that is opposite to that seen for the optical gap. Therefore, there exists a monotonic relation between  $E_0$  and the  $E_{04}$  gap (or Tauc gap), with  $E_0$  decreases at increasing optical gap. This observation is in contrast to that reported by Conde *et al.*<sup>14</sup> The Urbach tail width  $E_0$  is a measure of disorder in the materials and is expected to increase for  $a\text{-Si}_{1-x}\text{C}_x\text{:H}$  films containing a mixture of  $sp^2$  and  $sp^3$  phases. For  $a\text{-Si:H}$ ,  $E_0$  is typically  $\sim 50\text{ meV}$ ,<sup>39,40</sup> however, for  $a\text{-Si:H}$  alloys,  $E_0$  has been observed to be higher,<sup>39,41</sup> due to structural disorder as well as compositional disorder

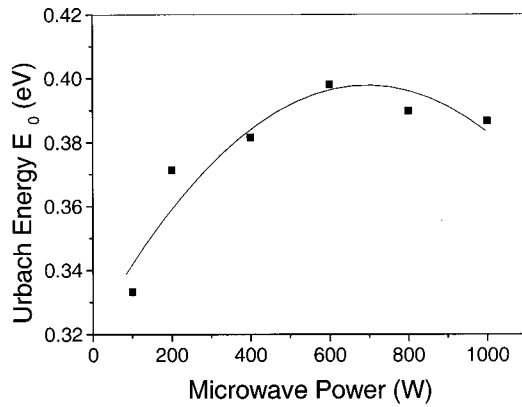


FIG. 6. The Urbach energy  $E_0$  as a function of microwave power.

as a result of alloying and hydrogenation. In this work, the increase in  $E_0$  from SCJ01 to SCJ04 can be related to the increasing carbon  $sp^2$  bond as illustrated by the Raman spectra, as this increases the overall structural disorder in the tetrahedrally bonded structure. For samples SCJ05 and SCJ06, the decrease in  $E_0$  can be accounted for by the tetrahedrally bonded Si-C bond seen in the FTIR spectra. The relatively low  $E_0$  for the sample SCJ01 suggests that it has much less disorder compared to the other samples, and as explained earlier could be related to the similar starving plasma condition used. Further detailed comparison of the other physical and electrical properties between the sample SCJ01 and those  $a$ -SiC:H deposited using a low density rf plasma is necessary before a conclusion can be drawn on how the ECR-CVD plasma at 100 W in our case compares with the low density rf plasma. Nevertheless, it is certain that the former has a higher ionization fraction, and the films deposited exhibit strong PL that resembles those seen in  $a$ -C:H films.

Figure 7 shows the normalized PL spectra for all the  $a$ -Si $_{1-x}$ C $_x$ :H films excited with an energy  $E_{ex}=3.41$  eV. The inset shows the variation of the PL peak emission energy  $E_{PL}$  as a function of the  $E_{04}$  gap. The  $E_{PL}$  is seen to increase with increasing  $E_{04}$  gap, spanning from 2.44 to 2.79 eV and corresponding to green to blue emission. Blue emission was first achieved from  $a$ -Si $_{1-x}$ C $_x$ :H by Nevin *et al.*,<sup>42</sup>

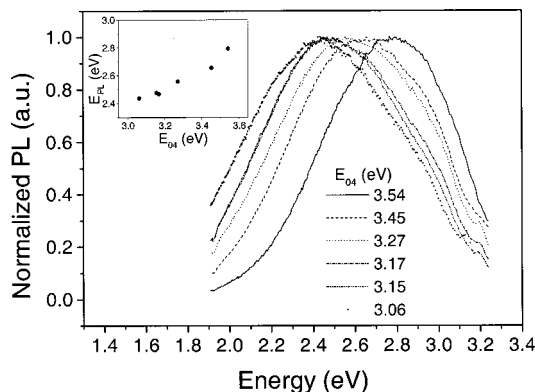


FIG. 7. The normalized PL spectra of the  $a$ -Si $_{1-x}$ C $_x$ :H films with various  $E_{04}$  gaps using  $E_{ex}=3.41$  eV. The inset shows the variation of the PL peak emission energy  $E_{PL}$  as a function of  $E_{04}$  gap.

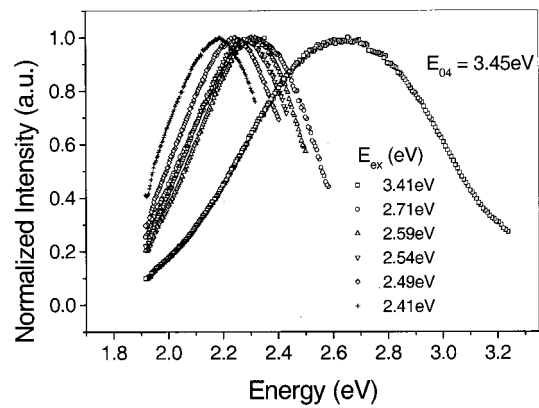


FIG. 8. The normalized PL spectra for the sample SCJ02( $a$ -Si $_{0.27}$ C $_{0.73}$ :H) at different excitation energies  $E_{ex}$ .

deposited using the rf-PECVD technique with silane and xylene as source gases. The  $E_{PL}$  was fixed at 2.61 eV despite varying excitation energy, attributed to radiative recombination of electron-hole pairs in localized states associated with the  $sp^2$ -carbon molecular orbitals of individual  $\pi$ -bonded units which remained constant throughout the range of samples.<sup>42</sup> However, in this work, the observed shift in  $E_{PL}$  with the  $E_{04}$  gap is believed to be dominated by the tail-to-tail states recombination, based on a model that has been generally accepted for PL in amorphous semiconductors such as  $a$ -Si:H and  $a$ -C:H.<sup>27,33</sup> In this model, photoexcited electron-hole pairs can radiatively recombine through localized band tail states or nonradiatively captured by defect centers. The PL critically depends on the width and the detailed structures of the density of the band tail states, which are usually strong functions of the microstructures of the films. In Si-rich  $a$ -Si $_{1-x}$ C $_x$ :H ( $x < x_c$ ), the PL is basically similar to that in  $a$ -Si:H,<sup>34</sup> arising from the radiative recombination of electrons and holes trapped in the band tail states.<sup>43</sup> PL is quenched by paramagnetic Si dangling bonds which act as nonradiative recombination centers.<sup>43,44</sup> In C-rich  $a$ -Si $_{1-x}$ C $_x$ :H ( $x > x_c$ ), the increase in the radiative recombination rate from PL lifetime  $\tau_r=10^{-3}-10^{-8}$  s<sup>45,46</sup> and the much larger Urbach tail width<sup>47</sup> give rise to PL observable at room temperature. In this work, the PL observed exhibits similar behavior to that observed in  $a$ -C:H<sup>27</sup> and is believed to be due to the carbon-rich polymeric nature of the films. The PL ranging from green to blue suggests that the  $a$ -Si $_{1-x}$ C $_x$ :H prepared by the ECR-CVD technique is a promising material for applications in large area flat panel displays. Towards that end, the PL efficiency of these films has to be further increased through optimization of the deposition conditions. Our recent work has shown that the PL efficiency of these ECR-CVD grown  $a$ -Si $_{1-x}$ C $_x$ :H films can be substantially increased when there are inclusion of SiC nanocrystallites.<sup>48</sup>

Figure 8 shows the normalized PL spectra at various  $E_{ex}$  for the sample SCJ02. It can be seen that  $E_{PL}$  increases with  $E_{ex}$ , which can be interpreted based on the tail-to-tail states recombination model, where the PL is derived from the thermalization and subsequent recombination of the carriers

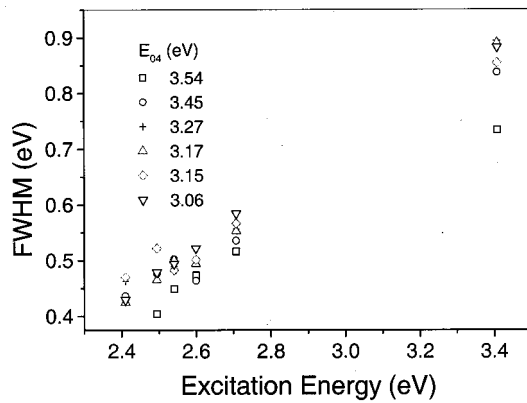


FIG. 9. The FWHM of the PL band as a function of the excitation energy  $E_{\text{ex}}$ .

across the tail states. At increasing  $E_{\text{ex}}$  that is below the mobility gap, localized states higher up in energy towards the band edges are involved in the electron hole pairs generating process. Therefore, the PL is derived from the recombination of carriers which span across a large part of the tail states, leading to photons with higher energy being emitted, and also over a wider range of energy. The latter is confirmed by the full width at half maximum (FWHM) of the PL spectra shown in Fig. 9, where it can be seen that for each film with a given  $E_{04}$  gap, the FWHM increases with  $E_{\text{ex}}$ . Similar behaviors have been observed for  $a$ -Si:H,<sup>49</sup>  $a$ -C:H,<sup>27</sup> and  $a$ -SiN<sub>x</sub>:H<sup>50</sup> and are general characteristics of PL in amorphous semiconductors with wide tail states.<sup>51</sup> In Fig. 9, it can be further seen that the film with the largest  $E_{04}$  gap (3.54 eV) exhibits smaller FWHM compared to the other films when excited at  $E_{\text{ex}} = 3.41$  eV. This is related to its smaller Urbach tail width  $E_0$  as can be seen in Fig. 10. Also, at increasing optical gap, the conduction and valence band tail states are generally separated further apart in energy. Therefore, for subgap excitation at a given  $E_{\text{ex}}$ , the states that are participating in radiative recombination are deeper down into the band tails, leading to less thermalization steps involved for the carriers and, hence, a smaller FWHM of the PL emission.

Figure 10 compares the PL FWHM values (at  $E_{\text{ex}} = 3.41$  eV) with the Urbach tail width  $E_0$ . It can be seen that

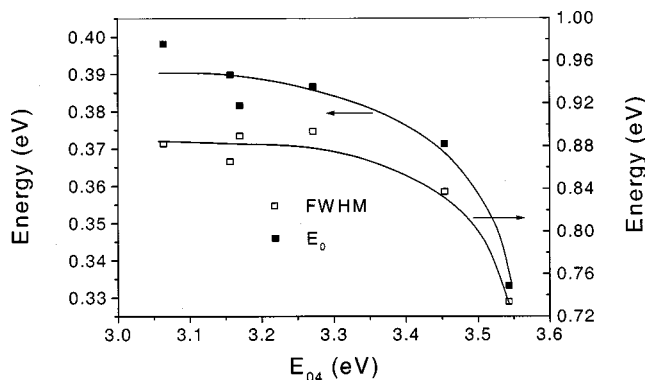


FIG. 10. The FWHM of the PL band at  $E_{\text{ex}} = 3.41$  eV and the Urbach energy  $E_0$  as functions of the  $E_{04}$  gap.

with increasing  $E_{04}$  gap, there is a slight decrease in both the FWHM and  $E_0$ . This is in contrast to the results reported for  $a$ -C:H,<sup>52</sup> where it was found that when the hydrogen content in the films was varied from 57.4% to 73.8%, an increase in the optical band gap, a narrowing of the tail width, and broadening of the luminescence band were observed. The results were interpreted in terms of the distribution of the carbon  $sp^2$  clusters density of states within the mobility gap.<sup>52</sup> According to this model, since the Tauc gap represents the average value of the cluster gap distribution, a larger Tauc gap therefore implies a wider distribution of cluster gaps taking part in the PL process, resulting in a broader bandwidth. However, this model is unlikely to account for the roughly linear relationship between the FWHM of the PL band and the Urbach energy observed in this work. In  $a$ -Si:H and its alloys such as  $a$ -Si<sub>1-x</sub>C<sub>x</sub>:H and  $a$ -SiN<sub>x</sub>:H, an increase in the Urbach energy results in an increase in the width of the PL band ( $\sigma_L$ ), which is derived from both disorder broadening ( $\sigma_L$ )<sub>disorder</sub> and phonon broadening ( $\sigma_L$ )<sub>Stokes</sub> and can be expressed as<sup>51</sup>

$$(\sigma_L)^2 = (\sigma_L)_{\text{disorder}}^2 + (\sigma_L)_{\text{Stokes}}^2 \quad (1)$$

If we assume that the contribution from phonon broadening is small compared to disorder broadening, a linear correlation between the PL bandwidth and Urbach energy is expected. Based on the static disorder modeled by Dunstan and Boulitrop,<sup>53</sup> Searle and Jackson<sup>51</sup> have predicted that ( $\sigma_L$ )<sub>disorder</sub> is proportional to the Urbach energy in  $a$ -Si:H as

$$(\sigma_L)_{\text{disorder}} \approx 2.45E_0 \quad (2)$$

In the case of  $a$ -Si<sub>1-x</sub>C<sub>x</sub>:H, similar correlation has been observed by several groups.<sup>51,54</sup> Our results have also revealed that the FWHM is proportional to  $E_0$  with a proportional constant of 2.15, which therefore suggest that the broadening of the band tails is the main factor that contributes to the shape of the PL band observed.

#### IV. CONCLUSIONS

We have studied the optical, structural, and emission properties of  $a$ -Si<sub>1-x</sub>C<sub>x</sub>:H films deposited by the ECR-CVD technique at varying microwave powers. The film grown at 100 W is similar to those deposited using the rf-PECVD technique under the rf starving plasma condition which exhibit high optical band gap, high stoichiometry and low Urbach energy  $E_0$ . The films deposited at higher microwave powers are carbon-rich polymeric  $a$ -Si<sub>1-x</sub>C<sub>x</sub>:H with carbon fraction around 0.7, almost independent of the microwave power. On the PL, the peak emission energy  $E_{\text{PL}}$  was shifted to higher energy and the bandwidth was narrowed with increasing  $E_{04}$  gap. On the  $E_{\text{ex}}$  dependence of the PL,  $E_{\text{PL}}$  was shifted to higher energy and the bandwidth was broadened with increasing  $E_{\text{ex}}$ . These PL behaviors observed can be interpreted using the tail-to-tail states recombination model for amorphous semiconductors with wide tail widths. A linear correlation between the PL FWHM and the Urbach energy  $E_0$  has also been noted, suggesting that broadening of the band tails is the main factor that accounts for the shape of the PL band observed.

- <sup>1</sup>F. Demichelis, F. Giorgis, C. F. Pirri, and E. Tresso, *Philos. Mag. B* **71**, 1015 (1995).
- <sup>2</sup>Y. Hamakawa and H. Okamoto, *Mater. Res. Soc. Symp. Proc.* **242**, 651 (1992).
- <sup>3</sup>D. Kruangam, T. Endo, and W. Guang-Pu, *Jpn. J. Appl. Phys., Part 2* **24**, L806 (1985).
- <sup>4</sup>Y. Hamakawa, *Mater. Res. Soc. Symp. Proc.* **49**, 239 (1985).
- <sup>5</sup>V. Chu, J. P. Conde, J. Jarego, P. Brogueira, J. Rodriguez, N. Barradas, and J. C. Soares, *J. Appl. Phys.* **78**, 3164 (1995).
- <sup>6</sup>G. Leo, G. Galluzzi, G. Guattari, R. Vincenzoni, F. Demichelis, G. Crovini, C. F. Pirri, and E. Tresso, *J. Non-Cryst. Solids* **164–166**, 1035 (1993).
- <sup>7</sup>A. Desalvo, F. Giorgis, C. F. Pirri, E. Tresso, P. Rava, R. Galloni, R. Rizzoli, and C. Summonte, *J. Appl. Phys.* **81**, 7973 (1997).
- <sup>8</sup>C. Partha and D. U. Kumar, *Jpn. J. Appl. Phys., Part 2* **36**, L1426 (1997).
- <sup>9</sup>D. M. Bhusari and S. T. Kshirsagar, *J. Appl. Phys.* **73**, 1743 (1993).
- <sup>10</sup>K. Winer, *Appl. Phys. Lett.* **55**, 1759 (1989).
- <sup>11</sup>T. Watanabe, M. Tanaka, K. Azuma, M. Nakatani, T. Sonobe, and T. Shimada, *Jpn. J. Appl. Phys., Part 1* **26**, 1215 (1987).
- <sup>12</sup>S. F. Yoon, H. Yang, Rusli, J. Ahn, Q. Zhang, and T. L. Poo, *Diamond Relat. Mater.* **6**, 1683 (1997).
- <sup>13</sup>F. S. Pool, *J. Appl. Phys.* **81**, 2839 (1997).
- <sup>14</sup>J. P. Conde *et al.*, *J. Appl. Phys.* **85**, 3327 (1999).
- <sup>15</sup>E. S. Aydil, J. A. Gregus, and R. A. Fottscho, *J. Vac. Sci. Technol. A* **11**, 2883 (1993).
- <sup>16</sup>T. Futagi, M. Katsuno, N. Ohtani, Y. Ohta, H. Mimura, and K. Kawamura, *Appl. Phys. Lett.* **58**, 2948 (1991).
- <sup>17</sup>T. Futagi, N. Ohtani, M. Katsuno, K. Kawamura, Y. Ohta, H. Mimura, and K. Kitamura, *J. Non-Cryst. Solids* **137&138**, 539 (1991).
- <sup>18</sup>S. F. Yoon and J. Ahn, *J. Vac. Sci. Technol. A* **15**, 1832 (1997).
- <sup>19</sup>D. Kruangam, T. Toyama, Y. Hattori, M. Deguchi, H. Okamoto, and Y. Hamakawa, *J. Non-Cryst. Solids* **97&98**, 293 (1987).
- <sup>20</sup>Y. Matsumoto, G. Hirata, H. Takakura, H. Okamoto, and Y. Hamakawa, *J. Appl. Phys.* **67**, 6538 (1990).
- <sup>21</sup>S. F. Yoon, R. Ji, J. Ahn, and W. I. Milne, *Diamond Relat. Mater.* **5**, 1371 (1996).
- <sup>22</sup>S. F. Yoon, R. Ji, and J. Ahn, *Philos. Mag. B* **77**, 197 (1998).
- <sup>23</sup>I. Solomon, M. P. Schmidt, and H. Tran-Quoc, *Phys. Rev. B* **38**, 9895 (1988).
- <sup>24</sup>M. N. P. Carreno, I. Pereyra, M. C. A. Fantini, H. Takahashi, and R. Landers, *J. Appl. Phys.* **75**, 538 (1994).
- <sup>25</sup>I. P. Xanthakis, *J. Non-Cryst. Solids* **164–166**, 1019 (1993).
- <sup>26</sup>J. Roberson, *Philos. Mag. B* **66**, 615 (1992).
- <sup>27</sup>Rusli, J. Robertson, and G. A. J. Amaratunga, *J. Appl. Phys.* **80**, 2998 (1996).
- <sup>28</sup>S. Z. Han, H. M. Lee, and H.-S. Kwon, *J. Non-Cryst. Solids* **170**, 199 (1994).
- <sup>29</sup>A. S. Kumbhar, D. M. Bhusari, and S. T. Kshirsagar, *Appl. Phys. Lett.* **66**, 1741 (1995).
- <sup>30</sup>W.-J. Sah, H.-K. Tsai, and S.-Ch. Lee, *Appl. Phys. Lett.* **54**, 617 (1989).
- <sup>31</sup>W.-J. Sah and S.-C. Lee, *Proceedings of the 2nd International Conference of Amorphous and Crystalline Silicon Carbide II*, 1991, p. 8588.
- <sup>32</sup>A. Chehaidar, R. Carles, A. Zwick, C. Meunier, B. Cros, and J. Durand, *J. Non-Cryst. Solids* **169**, 37 (1994).
- <sup>33</sup>J. Robertson, *Phys. Rev. B* **53**, 16302 (1996).
- <sup>34</sup>F. Tuinstra and J. L. Koenig, *J. Chem. Phys.* **53**, 1126 (1970).
- <sup>35</sup>M. Yoshikawa, G. Katagiri, H. Ishida, and A. Ishitani, *J. Appl. Phys.* **64**, 6464 (1988).
- <sup>36</sup>W. K. Choi, F. L. Loo, C. H. Ling, F. C. Loh, and K. L. Tan, *J. Appl. Phys.* **78**, 7289 (1995).
- <sup>37</sup>D. A. Anderson and W. E. Spear, *Philos. Mag.* **35**, 1 (1976).
- <sup>38</sup>R. Hillel, M. Maline, F. Gourbilleau, G. Nouet, R. Carles, and A. Mlayah, *Mater. Sci. Eng., A* **168**, 183 (1993).
- <sup>39</sup>W. B. Jackson and N. M. Amer, *Phys. Rev. B* **25**, 5559 (1982).
- <sup>40</sup>B. von Roedern, A. H. Mahan, T. J. McMahon, and A. Madan, *Mater. Res. Soc. Symp. Proc.* **49**, 167 (1985).
- <sup>41</sup>P. Fiorini, F. Evangelisti, and A. Frova, *Mater. Res. Soc. Symp. Proc.* **49**, 195 (1985).
- <sup>42</sup>W. A. Nevin, H. Yamagishi, M. Yamaguchi, and Y. Tawada, *Nature (London)* **368**, 529 (1994).
- <sup>43</sup>R. A. Street, *Hydrogenated Amorphous Silicon* (Cambridge University Press, Cambridge, 1991).
- <sup>44</sup>R. A. Street, J. Zesch, and M. J. Thompson, *Appl. Phys. Lett.* **43**, 672 (1983).
- <sup>45</sup>W. Siebert, R. Carius, W. Fuhs, and K. Jahn, *Phys. Status Solidi B* **140**, 311 (1987).
- <sup>46</sup>S. V. Chernsychev, E. I. Terukov, V. A. Vassilyev, and A. S. Volkov, *J. Non-Cryst. Solids* **134**, 218 (1991).
- <sup>47</sup>R. S. Sussmann and R. Ogden, *Philos. Mag. B* **44**, 137 (1981).
- <sup>48</sup>M. B. Yu, Rusli, S. F. Yoon, J. Cui, K. Chew, J. Ahn, and Q. Zhang, *International Conference on Metallurgical Coatings and Thin Films 2000*, San Diego.
- <sup>49</sup>S. Q. Gu, M. E. Rikh, and P. C. Taylor, *Phys. Rev. Lett.* **69**, 2697 (1992).
- <sup>50</sup>I. G. Austin, W. A. Jackson, T. M. Searle, P. K. Bhatt, and R. A. Gibson, *Philos. Mag. B* **52**, 371 (1985).
- <sup>51</sup>T. M. Searle and W. A. Jackson, *Philos. Mag. B* **60**, 237 (1989).
- <sup>52</sup>S. Liu, S. Gangopadhyay, G. Sreenivas, S. S. An, and H. A. Naseem, *J. Appl. Phys.* **82**, 4508 (1997).
- <sup>53</sup>D. J. Dunstan and F. Boulitrop, *Phys. Rev. B* **30**, 5945 (1984).
- <sup>54</sup>C. Palsule, S. Gangopadhyay, D. Cronauer, and B. Schroder, *Phys. Rev. B* **48**, 10 804 (1993).